Effect of Polydispersity on Fluorescence Quenching in Micelles Formed by Telechelic Associative Polymers

Robert J. English,† Ian Ratcliffe,† Rowan-Louise Blanchard,† and Barry J. Parsons*,‡

Centre for Water-Soluble Polymers, The North East Wales Institute of Higher Education, Wrexham, LL11 2AW, UK, and Faculty of Health, Leeds Metropolitan University, Leeds, LS1 3HE, UK

Received October 25, 2006; Revised Manuscript Received July 3, 2007

ABSTRACT: Time-resolved fluorescence quenching studies, using pyrene as a probe for micellar environments in solutions of a telechelic associating polymer based on PEG with *n*-C_{12} (dodecyl) hydrophobic end groups, have been carried out to determine the aggregation number(s) of the micelles. At low [pyrene]/[hydrophobe] values, η, quencher-average aggregation numbers, N_q, calculated from the fitting of the fluorescence decay curves to the Infelta equation were found to decrease rapidly as η increased. By fitting the N_q vs η plots to a cubic curve [Warr, G. G.; Grieser, F. *J. Chem. Soc., Faraday Trans. 1* **1986**, *82*, 1813], this observation was shown to be consistent with a highly skewed, polydisperse distribution of micelle aggregation numbers, described by a weight-average aggregation number of 75 and a standard deviation of 86. For a given polymer concentration in the range 1.0−2.5 g dL^{-1}, the fluorescence decay curves did not produce parallel $\log(I/I_0)$ vs time plots, as would be expected for a monodisperse array of micelles. Instead, the plots showed a characteristic intersection. Simulation of these curves using Infelta-type equations could not reproduce this behavior, indicating that a more refined model may be needed. This detailed study of the distribution of aggregation number in associative telechelic polymers is discussed in the context of recent investigations [Meng, X.-X.; Russel, W. B. *Macromolecules* **2005**, *38*, 593], from which it is suggested that polydispersity of micelle size is to be expected as a normal feature of such systems.

Introduction

Associative polymers are soluble polymers containing a small number of solvophobic groups that cluster dynamically in selective solvents. Under appropriate conditions of polymer concentration and solvent environment, such interactions lead to the formation of a transient network that spans the system, thus providing a mechanism for viscosification and structuring. Such materials include, for example, water-soluble polymers bearing large hydrophobic substituents.[1] Hydrophobically associating polymers have enjoyed the greatest use industrially, particularly to control the rheology of aqueous formulations leading to enhanced processability or improved end-use application properties. Typical applications include paints, coatings, adhesives, agrochemicals, ceramics, pharmaceuticals, and personal care products.[1] Other developing areas of application include separation media for DNA analyses,[2] responsive delivery systems for the triggered release of drugs,[3] and in petroleum recovery.[4]

A key feature of water-soluble polymers bearing hydrophobic groups is their ability to self-assemble into micellar structures. Determination of the aggregation number has therefore become the focus of many studies, and this parameter is used to account for both properties such as the rheological behavior of associative polymers and the microstructure of polysoaps. Experimental determination of the aggregation number of associating polymers is also paramount, as this parameter is a key output of numerical simulations of the aggregation process.

The experimental techniques that have been used successfully to determine micellar aggregation numbers in polymers are static light scattering, small-angle neutron scattering, and fluorescence quenching of probes such as pyrene. Time-resolved fluorescence measurements have been particularly successful following the pioneering studies with surfactants[5−8] and have been applied to polysoaps,[9−12] urethane-coupled poly(ethylene oxide) end-capped with hydrophobic substituents,[13] poly(ethylene oxide-*b*-styrene) di- and triblocks,[14] random copolymers of 2-(acrylamido)-2-methylpropanesulfonate (AMPS) and dodecyl methacrylate (DMA),[15−17] and hydrophobically modified alkali swellable emulsion polymers (HASE).[18−21]

Telechelic associative polymers have hydrophilic backbones and hydrophobic end groups in which the latter aggregate to form spherical micelles. This aggregation, as well as their ability to form bridges between micelles, profoundly affects their macroscopic properties, particularly their rheological behavior. Telechelic polymers appear to provide thickening as a consequence of their high network connectivity, and the scaling of the low shear viscosity, η_0, is mirrored by a change in the scaling of the plateau modulus, G'_p. Telechelic polymers are of particular interest in that it is simpler to simulate their aggregation behavior dynamically[22] and so provide a means of correlating experimentally observable material properties to their simulated behavior over a range of length and time scales.

The aggregation numbers of telechelic polymers have been determined using a variety of methods, including steady-state[23] and time-resolved fluorescence,[24,25] static light scattering[26,27] small-angle neutron scattering,[28,29] dynamic light scattering/viscometry,[30] and ^{19}F NMR.[31] Most of these can yield values of average aggregation numbers—although which is measured depends on the selected method. In their theoretical thermodynamic approach to the numerical prediction of aggregation numbers of a series of telechelic PEGs end-capped with dodecyl, hexadecyl, and octadecyl hydrophobes, Meng and Russel[32] calculated the number- and weight-average aggregation numbers and compared them with experimental values obtained in the same study and those measured by others.[23,33,34] They predicted that the aggregation number would decrease with increase in

* To whom correspondence should be addressed.
† The North East Wales Institute.
‡ Leeds Metropolitan University.

10.1021/ma0624649 CCC: $37.00 © 2007 American Chemical Society
Published on Web 08/10/2007

the number of poly(ethylene oxide) segments in the backbone. In addition, they also found good agreement between the predicted values of the number-average aggregation number of the dodecyl end-capped polymers and those found from experiments involving static fluorescence measurements. The agreement between predicted weight-average and experimental weight-average values found in dynamic fluorescence experiments[33,34] was, however, less good, reflecting perhaps incomplete end-capping of the polymers.[32] The results of other dynamic fluorescence meaurements[24,25] were not used for the comparisons on the grounds that the quencher concentrations employed were too high.[32]

In time-resolved (dynamic) fluorescence studies of a probe and quencher in a monodisperse array of micelles, the aggregation number determined from an analysis of the Infelta-type decays[6−8] will be independent of quencher concentration. However, in polydisperse systems and where the residence time of the probe is short compared to the lifetime of the micelle (i.e., a "static process"), it is now well-established that the aggregation number (determined assuming a monodisperse distribution of micelle size) will depend on the concentration of quencher.[35,36] In such polydisperse systems, a "quencher average" aggregation number, N_q, is determined. In the limit of zero quencher concentration, a weight-average aggregation number can be obtained—although this may only be an indicative value. It may be more appropriate then to simulate fluorescence decays by using an actual or assumed distribution of micelle size, as has been applied to rodlike surfactant micelles.[37] In the case of polymeric systems, for example hydrophobically modified polyacrylates (HMPAs), the degree of polydispersity of the micellar domains has been estimated using time-resolved fluorescence quenching techniques.[38] However, there has been little, if any, detailed study into polydispersity in aggregation numbers of telechelic associating polymers. It is the purpose of this study, therefore, to investigate the effect of such polydispersity on the time-resolved fluorescence quenching of probe molecules in micelles formed by a well-characterized telechelic polymer derived from 35 kDa PEG completely end-capped with dodecyl (C_{12}) groups.

Experimental Section

Materials. Poly(ethylene glycol) (M_w 35 000 Da), isophorone diisocyanate, dibutyltin dilaurate, *n*-dodecanol, and pyrene (sublimed, 99%) were purchased from Sigma-Aldrich, Gillingham, UK, and were used without further purification. Toluene, hexane, and acetone were distilled under reduced pressure prior to use. Hexane and acetone were further dried over $MgSO_4$.

Polymer Synthesis. Poly(ethylene glycol) (50.0 g) and toluene (100 g) were weighed into a five-neck 1 L reaction vessel equipped with a mechanical stirrer, nitrogen inlet, and a Dean−Stark water trap, coupled to a Davies condenser. The resultant solution was heated to ∼130 °C by means of an external, temperature-programmable oil bath and the solvent allowed to distill from the reactor, thus removing water present in the polymer (∼2−3 mL) as an azeotrope. The contents of the reactor were then cooled to 80 °C, and dibutyltin dilaurate (50 mg) was added, followed by a large excess of isophorone diisocyanate (6 mol of isocyanate to 1 mol of PEG OH groups). The reaction was allowed to proceed for 3 h at 80−85 °C under a blanket of N_2. *n*-Dodecanol was then introduced (12 mol of alcohol to 1 mol of PEG OH groups), and the end-capping reaction was allowed to continue for a further 3 h, after which the polymer solution was cooled to 45 °C, before the addition of methanol (30 mL) to react off any remaining isocyanate. The crude polymer was collected at the pump following precipitation in an excess of cold hexane.

The polymer was purified via multiple reprecipitation from toluene into cold hexane in order to remove low molecular weight byproducts and residual reactants, followed by a final precipitation on cooling from dry acetone. The polymer was dried under vacuum at room temperature and then stored at 4 °C under nitrogen.

Analysis of the polymer by SEC [3 × Styrogel Mixed-Bed columns, LiBr (0.2%) in DMF, PEG standards] indicated the presence of only a small fraction of chain extended material: $\bar{M}_w$ 44 900 = Da, $\bar{M}_n$ = 33 700 Da.

Time-Resolved Fluorescence Measurements. Time-resolved fluorescence experiments involved excitation by a Q-switched Nd:YAG laser (JK Lasers 2000 Series) capable of delivering up to 1 J of energy at 1064 nm in pulses of 12 ns duration.[39] In these experiments, a laser pulse at 355 nm was used which delivered typically 0.7 mJ per pulse to a quartz cuvette of 1 cm × 1 cm cross section. Fluorescence from pyrene was collected at right angles to the excitation pulse. At the concentrations employed (up to 60 μM), where pyrene acts simultaneously as probe and quencher, less than 0.1% of the pyrene is converted to fluorescent excited states. In addition, the absorbance of solutions containing the probe were typically less than 0.01, thus providing a relatively uniform distribution of pyrene fluorescence across the exit face of the cuvette. A high-radiance monochromator, set at 380 nm with a bandwidth of 5 nm, was used to monitor the pyrene monomer fluorescence signal, which was captured by a R-928 photomultiplier and stored digitally for subsequent kinetic analysis.

Aqueous solutions of the polymer itself were found to exhibit a weak, very short-lived (∼15 ns) fluorescence, the origin of which was uncertain. However, for pyrene concentrations more than 10 μM, the contribution to the total emission intensity was less than ∼5%. In the case of the data presented below, this contribution fell within the noise of the signal. There was therefore negligible difference between the kinetic parameters determined for pyrene containing polymer solutions and the corresponding values calculated following subtraction of the contribution from polymer fluorescence.

Preparation of Polymer Solutions. Solutions for time-resolved fluorescence experiments were prepared by the addition of distilled water to an appropriate mass of polymer. Dissolution of the polymer was facilitated by subsequent roller mixing, typically for 24−48 h. A saturation technique was employed to introduce the pyrene probe into these solutions. The required amounts of a stock solution of pyrene in acetone (3.2 mM) were introduced into glass vials via a micropipet, and the solvent was removed under a stream of nitrogen. Polymer solution was then added and dissolution of the probe facilitated by roller mixing of the solutions for several days, after which the samples were agitated at 60 °C for 3 h. The cooled solutions were centrifuged (120 min, 2500 rpm) to remove undissolved pyrene. In order to prepare solutions in the desired range of pyrene concentrations (nominally 25−100 μM), the resultant supernatants were diluted quantitatively with appropriate amounts of pyrene-free polymer solution. These diluted solutions were equilibrated by roller mixing. The final pyrene concentration in each solution was determined spectroscopically by measurement of the absorbance at 337 nm in quartz cuvettes. The extinction coefficient of pyrene at this wavelength was taken as 3.58×10^4 M^{-1} cm^{-1}.

Dynamic Light Scattering from Aqueous Polymer Solutions. Aqueous solutions of the polymers (0.1 and 1.0 g dL^{-1}) were prepared by tumbling an appropriate quantity of the polymer with filtered (0.2 μm Anopore membrane) distilled water on a roller mixer for 2 days. These stock solutions were further diluted with filtered solvent to produce aqueous solutions in the concentration range 0.05−1.0 g dL^{-1} and equilibrated by roller mixing. Polymer concentrations were verified gravimetrically. Dynamic light scattering (DLS) experiments were performed on filtered (0.45 μm) samples at 25 °C using a Zetasizer 1000HS instrument (Malvern Instruments, Malvern, UK). The laser wavelength was 634 nm and the scattering angle 90° ($q = 4\pi n_s \sin(\theta/2)/\lambda = 1.01 \times 10^7$ m^{-1}). The resultant autocorrelation functions were analyzed using the CONTIN algorithm. At the lowest polymer concentrations, the single broad relaxation mode was attributed to the translational

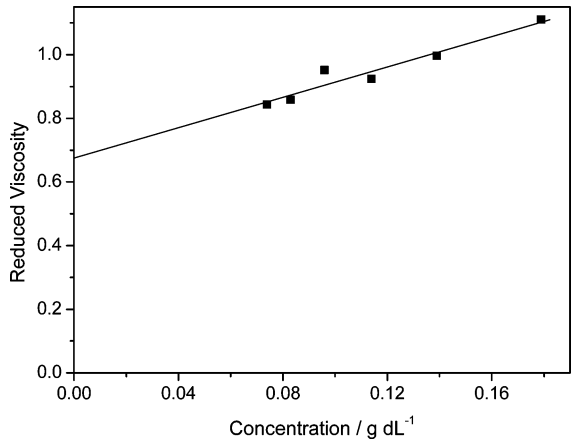

Figure 1. Huggins plot of reduced viscosity, η_{sp}/c, as a function of polymer concentration, c. Intrinsic viscosity, $[\eta]$, = 0.66 dL g^{-1}, Huggins coefficient, k', = 5.3.

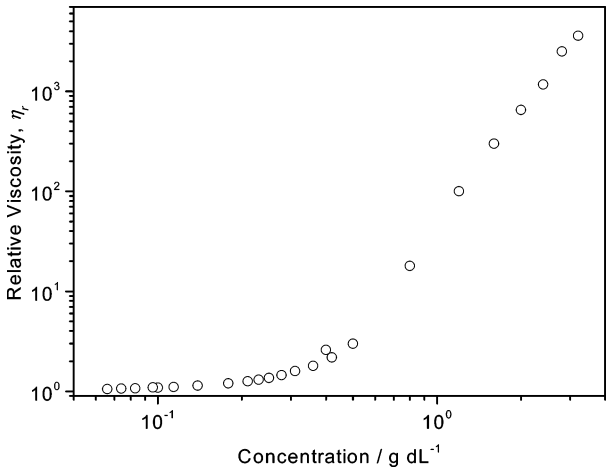

Figure 2. Variation of the zero shear relative viscosity of aqueous solutions of the polymer as a function of concentration. Photophysical studies were conducted on solutions in the concentration range c = 1.0−2.5 g dL^{-1}, where the viscosity increases strongly—this corresponds to the percolated regime associated with the existence of an infinite supramicellar network.

diffusion of the flower micelles, as discussed below. However, at higher concentrations more complex modes of relaxation were apparent.

Viscometry. The intrinsic viscosity of the polymer was determined by U-tube viscometry. Polymer solutions were prepared in an identical manner to that in the light scattering experiments described above. Measurements were made at 25.0 ± 0.1 °C using a Cannon 75 capillary dilution viscometer (Cannon Instrument Co., State College, PA). Selected solutions prepared at higher concentrations were characterized using a rotational rheometer (TA Instruments, AR2000) fitted with a concentric cylinder geometry.

Results and Discussion

Dynamic Light Scattering and Viscometry Measurements. Viscometry data are shown as the customary Huggins plot of reduced viscosity, η_{sp}/c, as a function of polymer concentration, c, in Figure 1. The data are well described by the Huggins equation, which is usually written in the form

$$\frac{\eta_{sp}}{c} = [\eta] + k_h[\eta]^2 c + ... \quad (1)$$

$[\eta]$ being the intrinsic viscosity and k_h the Huggins coefficient. The intrinsic viscosity of the polymer in water was determined to be 0.66 ± 0.3 dL g^{-1} (0.066 ± 0.003 m^3 kg^{-1}). Pham et al. reported values of $[\eta]$ = 0.47 and 0.51 dL g^{-1} for C_{16} and C_{18} end-capped 35 kDa PEG, respectively.[30] However, these materials were prepared via direct end-capping with the corresponding alkyl isocyanate, so were completely free of chain extended material. Alami et al. reported $[\eta]$ = 0.35 dL g^{-1} for a C_{12} end-capped PEG of lower molar mass (20 kDa).[33] For simple homopolymers in a thermodynamically "good" solvent, the value of k_h is usually around ∼0.3, increasing to ∼0.7 at the θ condition. A value of k_h of 0.3 ± 0.1 has been previously reported for 35 kDa PEG,[30] although there has been considerable variation in the results cited by different workers. For telechelic associating polymers, k_h usually greatly exceeds this latter value and may be interpreted as a binary interaction parameter describing the strength of the intermicellar bridging attraction. In the present case, k_h was found to be ∼5.3. Values of k_h in excess of ∼12 have been reported for telechelic polymers with long chain alkyl hydrophobes (C_{18}).[30]

The concentration dependence of the relative viscosity of aqueous solutions of the polymer is depicted in Figure 2. These data span the dilute regime to the percolated regime, where the viscosity increases rapidly. Mechanistically, viscosification is envisaged to involve formation of supramolecular clusters as a consequence of intermicellar bridging. As the volume occupancy of the micelles, ϕ, increases, bridging interactions increase in number and a polydisperse array of larger clusters are formed. The lifetime of a given cluster is likely to be much shorter than the hydrodynamic relaxation time of a single micelle; hence, these structures are by their nature highly transient. The process of cluster growth continues through the percolation threshold, c^*, where an infinite, sample-spanning cluster is formed. If one considers that $c^* \sim 0.4$ g dL^{-1} from the inflection in the relative viscosity curve, then the corresponding volume occupancy of the flower micelles[30] is $\phi^* = c^*[\eta]/2.5 \sim 0.11$. The photophysical experiments described below were carried out at concentrations between 1.0 and 2.5 g dL^{-1}. This corresponds to $c > c^*$, suggesting the presence of an infinite supramicellar network under these conditions.

The intensity-weighted distributions of the relaxation times determined from DLS experiments at various polymer concentrations are plotted in Figure 3. By reference to the comprehensive study of Alami et al. concerning a C_{12} end-capped 20 kDa PEG, each of the relaxation modes observed in aqueous solutions of telechelic associating polymers of this type is expected to be diffusive in character over the concentration range studied ($\Gamma \sim q^2$).[33] It is now useful to benchmark the results of the present study against these previous results. At the lowest concentrations shown in Figure 3 ($c > 0.1$ g dL^{-1}), a single broad relaxation mode is apparent. This typically spans almost a decade of relaxation times. Results were reproducible run-to-run and on repeating with freshly prepared samples. By reference to previous studies on similar telechelic polymers,[32] the most appropriate assignment to this relaxation process is the diffusion of discrete flower micelles.[34] Alami et al. noted an equivalent relaxation mode with an apparently similar concentration dependence and distribution of time scales.[30] However, these authors also noted a much faster mode (<50 μs), assigned to diffusion of unimers or oligomeric aggregates. In the present study, this "unimers" mode appears to be absent. At around c = 0.4 (Figure 3) the distribution of relaxation times becomes broader and more complex, with a suggestion of a shoulder at shorter times. This corresponds to the point at which viscometric measurements suggest the formation of a rheologically significant network (Figure 2).

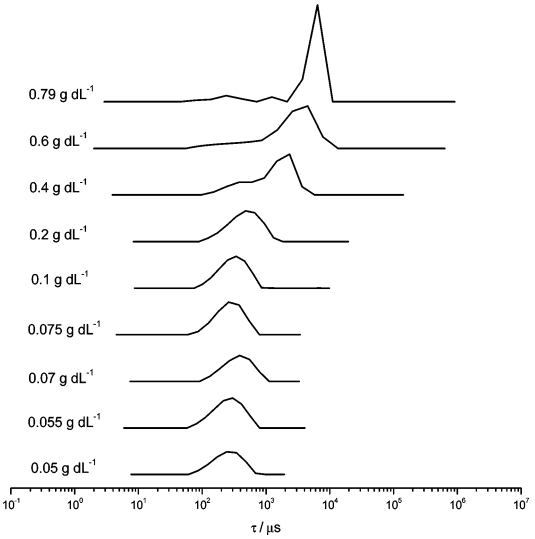

Figure 3. Intensity-weighted distributions of the hydrodynamic relaxation times determined by dynamic light scattering at various polymer concentrations. The single, relatively broad, mode at lower concentrations is assigned to the diffusion of single flower micelles. Photophysical studies were conducted in the percolated regime at higher concentrations (c = 1.0−2.5 g dL^{-1}), where the data suggest more complex cooperative diffusion within the interconnected network.

The concentration dependence of the apparent diffusion coefficient of the flower micelles, D_{app}, is commonly described by

$$\frac{D_{app}}{D_{0,app}} = 1 + k_d c[\eta]... \quad (2)$$

where k_d may be interpreted as a hydrodynamic virial coefficient. The infinite dilution value, $D_{0,app}$, was determined to be 8.14 × 10^{-12} m^2 s^{-1}. The value of k_d provides another measure of the strength of the intermicellar bridging attraction, in a manner analogous to k_h above. Intermicellar bridging imparts a negative value to the second virial coefficient, which is in turn reflected in a strongly negative k_d. In the present case, k_d was found to be −3.8. Pham et al. noted corresponding values of −4.3 and −6.8 respectively for C_{16} and C_{18} end-capped 35 kDa PEG; however, these polymers lacked the isophorone bridging moieties present in the polymer of the present study.

Dynamic Fluorescence Measurements. Aqueous solutions of the telechelic polymer at concentrations ranging from 1.0 to 2.5 g dL^{-1}, containing up to 60.3 μM pyrene, were excited at 355 nm as described above and the fluorescence emission monitored typically for about 1200 ns following the pulse. Most experiments were conducted using air-saturated solutions, to avoid foaming on purging with N_2 and loss of pyrene (presumably due to deposition on the side of the cuvette on purging). Where comparative experiments were performed both in air and with deaerated solutions, no significant differences in the apparent aggregation numbers or intramicellar quenching rate constants were found (see below). However, differences in the rate of fluorescence decay of the excited pyrene monomer were observed, as expected. In solutions that had been deaerated, the fluorescence decay rate from excited pyrene monomers (measured in 1.0 g dL^{-1} polymer solutions containing 4.4 μM pyrene) was (3.6 ± 0.03) × 10^6 s^{-1}. This value is comparable with the corresponding rates found for pyrene solubilized in micelles of $C_{12}EO_8$, where values of (2.7−3.3) × 10^6 s^{-1} were obtained.[40] In aerated solutions of 1.0 g dL^{-1} polymer and 4.4 μM pyrene, the rate of monomer fluorescence decay increased to (4.6 ± 0.03) × 10^6 s^{-1}. This value can be compared to values obtained for $C_{12}EO_8$ in aerated solutions which ranged from 4.0 × 10^6 to 6.1 × 10^6 s^{-1} and which increased with temperature in the range 15−35 °C, although this latter effect was not discussed by the authors.[40]

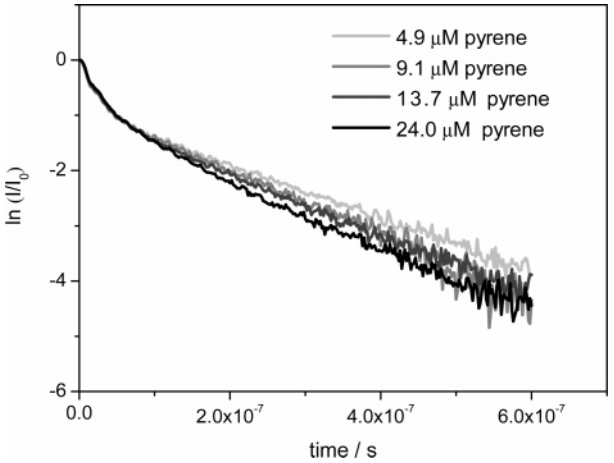

Figure 4. Fluorescence decay curves from aqueous polymer solutions containing various concentrations of pyrene (polymer concentration, c = 1.0 g dL^{-1}).

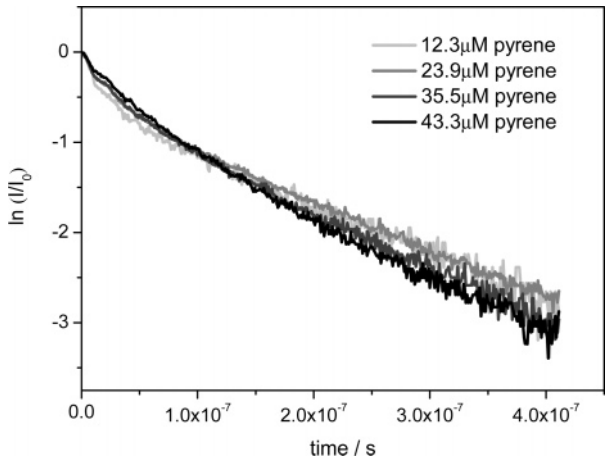

Figure 5. Fluorescence decay curves from aqueous polymer solutions containing various concentrations of pyrene (polymer concentration, c = 1.5 g dL^{-1}).

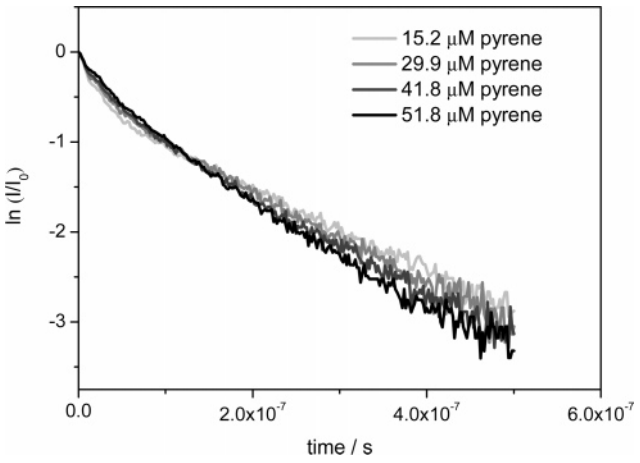

Figure 6. Fluorescence decay curves from aqueous polymer solutions containing various concentrations of pyrene (polymer concentration, c = 2.0 g dL^{-1}).

Figures 4−7 show the effect of variation in pyrene concentration on the fluorescence decays for aerated polymer solutions

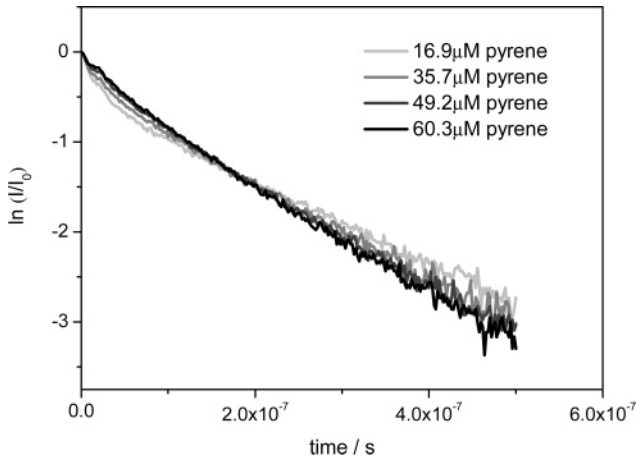

Figure 7. Fluorescence decay curves from aqueous polymer solutions containing various concentrations of pyrene (polymer concentration, $c = 2.5$ g dL^{-1}).

increasing in concentration from 1.0 to 2.5 g dL^{-1}, respectively. The kinetic data are presented in terms of the temporal evolution of $\ln(I_t/I_0)$ following the excitation pulse, I_t and I_0 being the fluorescence intensities at time t and $t = 0$, respectively. Each plot is typically the average of between 2 and 4 experiments and is shown for the first 600 ns of the fluorescence decay for clarity. A similar effect of increasing pyrene concentration is observed for each polymer concentration. That is, the set of decay curves in each of Figures 4−7 shows a "crossover" or common intersection between 100 and 200 ns after the laser pulse, which is somewhat unusual. This intersection becomes more obvious at higher polymer concentrations. For monodisperse micelles, a series of curves which do not cross and which have parallel slopes at longer times are expected, as the concentration of quencher is increased. Nevertheless, each of the plots in Figures 4−7 was found to fit the following Infelta eq 3 which has been developed previously for the general case of an immobile fluorescent probe and mobile quencher, both of which are located in a monodisperse array of micelles and where it is assumed that occupation of micelles by the probe and quencher obeys a Poisson distribution:[6−8,41]

$$I_t = I_0 \exp[-A_2 t + A_3 (\exp(-A_4 t) - 1)] \qquad (3)$$

where

$$A_2 = k_0 + \frac{k_q k_- n}{k_- + k_q}$$

$$A_3 = \frac{n k_q^2}{(k_q + k_-)^2}$$

$$A_4 = k_q + k_-$$

and where k_0 is the rate of decay of pyrene monomer fluorescence, k_q is the rate of intramicellar quenching by pyrene, k_+ is the second-order rate constant for entry of a quencher into a micelle, k_- is the rate of exit of the quencher from the micelle, and n is the average number of quenchers per micelle.

In the case where quencher (and probe) do not leave the micelle during the lifetime of the excited probe, the above equations reduce to $A_2 = k_0$, $A_3 = n$, and $A_4 = k_q$. Migration of the quencher during the lifetime of the excited probe is assumed to take place when A_2 is greater than k_0 and also increases with the concentration of quencher. However, it is probably necessary to monitor the fluorescence decay over 6−7 excited probe lifetimes to demonstrate, with confidence, that migration of the quencher or probe is occurring.[9] Furthermore, it has been shown that systems in which the micelles are polydisperse may also exhibit similar behavior on increasing the quencher concentration.[9,37]

The experimental data in Figures 4−7 were subsequently fitted to eq 3, and the resultant kinetic parameters are summarized in Table 1, together with the correlation coefficient (R^2) as an indicator of "goodness of fit". Also shown are the corresponding η values (η = [pyrene]/[hydrophobe]) and the so-called "quencher average" hydrophobe aggregation numbers, N_q. Calculation of the latter parameter is based on the following expression, the original derivation being based on an assumed monodisperse array of micelles:

$$N_q = \frac{[\text{hydrophobe}]n}{[\text{pyrene}]} \qquad (4)$$

Equation 4 implies that a linear plot of n vs [pyrene] would, for a fixed [hydrophobe], have a slope equal to the aggregation number, N_q, and a zero intercept.

A number of observations are immediately apparent from Table 1. First, the values of A_2 ($(4.5-6.4) \times 10^6$ s^{-1}) are similar in magnitude and range to those found for $C_{12}EO_8$ solutions in air.[40] There is little evidence that A_2 increases with increase in pyrene concentration—any effect would be small (see Figure 8). If all A_2 values are considered, regardless of polymer concentration, there is no discernible effect attributable to variation in the concentration of pyrene. Any variation in A_2 is, therefore, more likely attributable to variations in the concentration of oxygen concentration in the micelle. In deaerated solutions, lower values of A_2 are generally observed [$(3.6-4.1) \times 10^6$ s^{-1} (Table 1)], consistent with values found for $C_{12}EO_8$ solutions ($(2.8-3.3) \times 10^6$ s^{-1}).[40] It should also be noted that for both aerated and degassed solutions of $C_{12}EO_8$ similar aggregation numbers were measured.[40] Given the difficulties in degassing the polymer solutions used in this study, where foaming was prevalent, there is insufficient evidence to establish an effect of pyrene concentration on A_2. Such an effect, if found to be linear, can be used to indicate that migration of the probe out of the micelle within the excitation lifetime is taking place. However, it is usually difficult to establish that migration is occurring in this manner—requiring measurements of A_2 to be made over at least 5−6 lifetimes.[9] Moreover, an apparent effect of probe concentration on A_2 may be anticipated if there is significant polydispersity in micelle size.[35]

Second, the values of A_4 show a much more distinct dependence on pyrene concentration as further highlighted in Figure 9. Here, it appears that A_4 decreases from about 4.0×10^7 s^{-1} at low pyrene concentration to about 1.0×10^7 s^{-1} at high pyrene concentration ($\eta = 0.05$). For the sake of clarity, the data in Figure 9 are fitted to a linear relationship from which it appears that the effect is identical, within likely experimental error, for all polymer concentrations.

Third, N_q values show a significant inverse relationship with pyrene concentration; these are plotted against η in Figure 10. It is the latter observation that is the most significant. It has already been established that such "quencher average" aggregation numbers, derived from fitting probe fluorescence decay curves to the Infelta equation, will show an inverse dependence on η for a polydisperse array of micelle size.[35,36] The above relationship should hold particularly in the case of low η values (0−0.05),[35,36] i.e., a similar range to that of this study. This hypothesis arises from several assumptions: (i) that the mean number of probes or quenchers in a micelle is proportional to

Table 1.

c/g dL^{-1}	[pyrene]/μM	η	gas	10^6A_2/s^{-1}	A_3	10^7A_4/s^{-1}	R^2	N_q
1.0	9.1	0.016	air	5.96 ± 0.06	0.80 ± 0.02	4.07 ± 0.50	0.984	50.1
1.0	13.7	0.024	air	5.49 ± 0.08	0.96 ± 0.04	2.89 ± 0.57	0.953	39.9
1.0	24	0.042	air	5.70 ± 0.05	1.13 ± 0.02	1.77 ± 0.09	0.994	26.8
1.5	12.3	0.014	air	5.43 ± 0.06	0.61 ± 0.02	3.97 ± 0.39	0.979	42.4
1.5	23.9	0.028	air	5.26 ± 0.03	0.61 ± 0.01	2.56 ± 0.09	0.997	21.8
1.5	35.5	0.041	air	5.77 ± 0.06	0.65 ± 0.02	1.97 ± 0.12	0.994	15.7
1.5	43.3	0.051	air	5.68 ± 0.12	0.83 ± 0.05	1.04 ± 0.75	0.995	16.4
2.0	15.2	0.013	air	4.76 ± 0.04	0.55 ± 0.02	4.07 ± 0.60	0.987	41.3
2.0	29.9	0.026	air	5.04 ± 0.06	0.54 ± 0.03	2.55 ± 0.45	0.979	20.6
2.0	41.8	0.037	air	4.68 ± 0.08	0.80 ± 0.04	1.05 ± 0.11	0.989	21.8
2.0	51.8	0.045	air	5.27 ± 0.13	0.71 ± 0.07	0.97 ± 0.17	0.981	15.6
2.5	16.9	0.012	air	4.52 ± 0.03	0.54 ± 0.01	3.29 ± 0.29	0.994	45.5
2.5	35.7	0.025	air	5.28 ± 0.05	0.39 ± 0.02	3.10 ± 0.75	0.982	15.6
2.5	49.2	0.034	air	5.50 ± 0.06	0.37 ± 0.03	1.71 ± 0.34	0.989	10.7
2.5	60.3	0.042	air	5.56 ± 0.09	0.43 ± 0.05	1.04 ± 0.22	0.989	10.2
1.5	12.3	0.014	N_2	3.55 ± 0.03	0.70 ± 0.01	3.39 ± 0.11	0.993	48.7
1.5	23.9	0.028	N_2	4.11 ± 0.03	0.65 ± 0.01	2.62 ± 0.82	0.996	23.3
1.5	35.5	0.041	N_2	3.98 ± 0.05	0.81 ± 0.02	1.71 ± 0.07	0.991	19.5
1.5	43.3	0.051	N_2	4.66 ± 0.05	0.58 ± 0.02	1.36 ± 0.58	0.998	11.5
2.0	15.2	0.013	N_2	3.66 ± 0.02	0.59 ± 0.01	3.62 ± 0.27	0.993	44.3
2.0	41.8	0.037	N_2	6.11 ± 0.08	0.36 ± 0.02	3.43 ± 0.65	0.987	9.8

the aggregation number, (ii) the number of quencher molecules in a micelle is independent of the presence of a probe molecule (and vice versa), and (iii) that quenching of fluorescence occurs in the static limits; i.e., there is no exchange of probe and quencher in or out of micelles during the lifetime of the excited probe.[35,36] Progressive addition of quencher molecules will force the quencher to become more evenly distributed across the complete set of micelles. As a result, the experimentally determined aggregation number, calculated assuming a monodisperse array of micelle size, will show a dependence on quencher concentration.

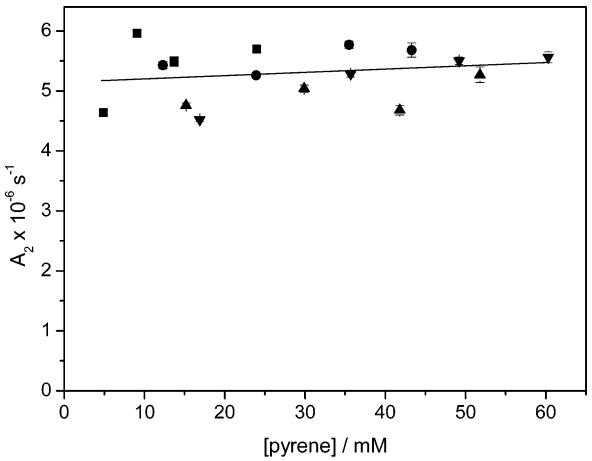

Figure 8. Variation in the unimolecular emission rate constant, A_2 ($=k_0$), as a function of pyrene concentration. Data are shown for aqueous solutions containing various concentrations of polymer: ■, c = 1.0 g dL^{-1}; ▲, c = 1.5 g dL^{-1}; ▼, c = 2.0 g dL^{-1}; ●, c = 2.5 g dL^{-1}.

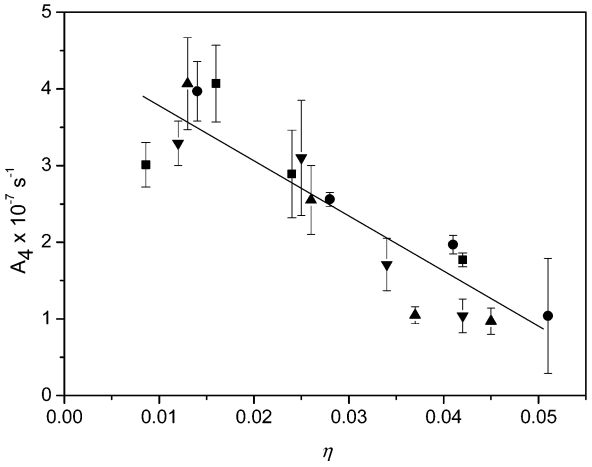

Figure 9. Variation in the intramicellar quenching rate constant, A_4 ($=k_q$), as a function of normalized pyrene concentration, η (= [pyrene]/[hydrophobe]). Data are shown for aqueous solutions containing various concentrations of polymer: ■, c = 1.0 g dL^{-1}; ●, c = 1.5 g dL^{-1}; ▲, c = 2.0 g dL^{-1}; ▼, c = 2.5 g dL^{-1}.

Similarly, the intramicellar quenching rate constant (A_4) may also depend on quencher concentration, since the rate of quenching will be expected to decrease as micelle size increases. Increasing the pyrene concentration should modify the distribution of occupied micelles, depending on their number and size, and hence the aggregated quenching rate constants arising from the polydisperse distribution micelle size should change with [pyrene].[35,36,41]

From the shape of the curve in Figure 10, it is clear that that N_q does indeed show an inverse relationship with η, but one which is not linear. It is unlikely therefore that there is a symmetrical Gaussian-type distribution of micelle size, but instead it is probable that it is a skewed or an exponential one.[36,37] The shape of the curve in Figure 10 can be fitted to the following equation appropriate to a triangular, exponential, or skewed Gaussian distribution:[36,37]

$$N_q = N_w - \frac{\sigma^2\eta}{2} + \frac{\Lambda\eta^2}{6} + \frac{E\eta^3}{24} \tag{5}$$

Here, N_w is the weight-average aggregation number, σ is the root-mean-square deviation of the distribution, and Λ and E are the raw skewness and kurtosis of the distribution, respectively. A reasonable fit (R^2 = 0.81), with no stationary points, of the above equation to the data in Figure 10 was obtained by regression analysis. This yielded values of N_w = 75, σ = 86, Λ = 373 000, and E = 7 650 000. Using the same treatment adopted by Warr and Grieser,[36] the skewness and kurtosis were standardized with respect to a Gaussian distribution using the following relationships:

$$\lambda = \frac{\Lambda}{2\sigma^3} \tag{6}$$

$$\epsilon = \frac{1}{8}\left[\left(\frac{E}{\sigma^4}\right) - 3\right] \tag{7}$$

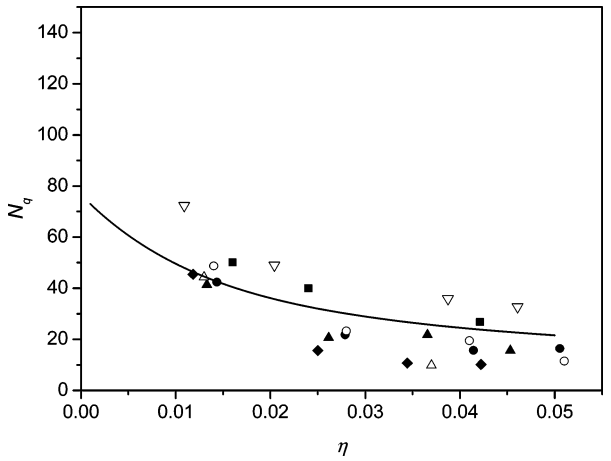

Figure 10. Variation in the quencher average hydrophobe aggregation number, N_q, as a function of normalized pyrene concentration, η (= [pyrene]/[hydrophobe]). Data are shown for aqueous solutions containing various concentrations of polymer: ■, c = 1.0 g dL^{-1} (air); ●, c = 1.5 g dL^{-1} (air); ▲, c = 2.0 g dL^{-1} (air); ◆, c = 2.5 g dL^{-1} (air); ○, c = 1.5 g dL^{-1} (N_2 purged); △, c = 2.0 g dL^{-1} (N_2 purged); ▽, data from Vorobyova et al.[24] c = 0.21 g dL^{-1} (air) [35 kDa PEG C_{16}]. The curve is a representative fit to the experimental data calculated using eqs 8 and 10; see text.

Note that $\lambda > 0$ denotes positive skewness (mean > mode, i.e., a distribution with an asymmetric tail extending to higher micelle size) and $\epsilon > 0$ means that the distribution is more peaked than a Gaussian one. Using this approach, $\lambda = 0.29$ and $\epsilon = -0.36$. The latter are consistent with the range of values found for various model, skewed distributions where values for λ ranged from 0.011 to 0.910 and where values ϵ of ranged from −0.162 to −0.392.[36] From this treatment, therefore, it would appear that the polymer solutions used in this study exhibit a high degree of polydispersity in micelle size (hydrophobe aggregation number). In addition, the distribution of micelle sizes has a positive skewness; i.e., the distribution of the aggregation number is skewed to lower values and has an asymmetric tail extending to larger aggregation numbers. The relatively high value of 86 for the standard deviation would indicate that the mean aggregation number is low—less than ∼20 (defined in terms of the number of hydophobes, each telechelic polymer contributing two hydrophobes to the micelle core)—and that there is a "long tail" in the distribution extending well beyond the weight-average aggregation number, N_w, of 75.

In an alternative approach, Warr and Grieser used the following expression to calculate the quencher average aggregation number, N_q:

$$N_q = \frac{1}{\eta}\frac{\sum f(N)N}{\sum f(N)Ne^{-\eta N}} \tag{8}$$

where $f(N)$ is the probability distribution function of micelle size and N is the micelle aggregation number. This equation can, in principle, be fitted to the experimental data in Figure 10. Two approaches were taken here.

In the first, the theoretical slightly skewed polydisperse distribution determined by Meng and Russel for a C_{16} end-capped 35 kDa telechelic polymer[32] was approximated by the equation

$$f(N) = \left[\frac{1}{(N_1 - N_2)}\right][\exp(-(N-1)/N_1) - \exp(-(N-1)/N_2)] \tag{9}$$

where N_1 and N_2 are 20 and 10, respectively.

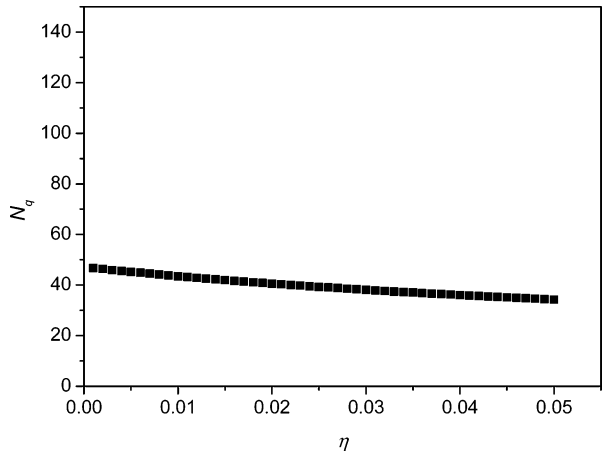

Figure 11. Calculated quencher average aggregation number, N_q, as a function of normalized pyrene concentration, η (= [pyrene]/[hydrophobe]) for a predicted distribution of micelle aggregation numbers using the approach of Meng and Russel[32] (eqs 8 and 9; see text).

Equations 8 and 9 were then used to calculate N_q as a function of η, where $f(N)$ was calculated for N values up to 300. The resultant plot is shown in Figure 11. It can be seen that N_q decreases from a weight-average aggregation number, N_w, of about 47, at $\eta = 0$, to about 34, at $\eta = 0.05$. It is clear, therefore, that the experimental N_q values in Figure 10 cannot be fitted closely by this particular probability distribution function as it is not sufficiently skewed.

In a second approach, a number of skewed distributions were selected in a "trial and error" attempt to use eq 8 to fit the data of Figure 10. It became clear that, in order to get sufficient curvature of the N_q vs η curve at low η values, it was necessary to adopt exponential distributions that had a "long tail" at high N values. A typical fit of this type is given (in Figure 10) by the following exponential distribution (for N up to 300).

$$f(N) = 0.2[\exp(-(40 - N)/5) + \exp(-(60 - N)/100)] \tag{10}$$

Such a distribution is very skewed relative to the theoretical one developed by Meng and Russel, and numerically, the greatest proportion of micelles have aggregation numbers between 2 and 30, reflected by a mean aggregation number of 10.3 and a standard deviation of 165, calculated from eq 10. Both the experimental data and the fit (from eqs 8 and 10) in Figure 10 are consistent with a weight-average micelle size, N_w, of about ∼84 hydrophobes.

Attempts were also made to simulate numerically the effect of polydispersity in aggregation number on the rate of pyrene quenching in these polymer solutions. This approach involved estimating the fractional contribution of micelles of a given size within the distribution to the experimentally observed decay curve of pyrene fluorescence, using the approach demonstrated previously by Almgren and co-workers for micelles of low molar mass surfactants.[35,37] Essentially, the modeling requires an assumed distribution of "micelle size" (i.e., aggregation number, N) and also an empirical equation that allows the calculation of the intramicellar quenching rate constant ($A_4 = k_q$) as a function of N. (The approach developed by Almgren equation uses an inverse relationship between the quenching rate constant, k_q, and N and N^2.) It is then assumed that the probability of a quencher occupying a micelle is proportional to the product of N and $f(N)$, the latter being the micelle size distribution function. In this way, the contribution of each Infelta-type decay from an array of micelles of a particular size to the total aggregated

Infelta-type decay arising from all micelle sizes can be weighted and summed.

As a start, to analyze our data, a similar skewed distribution to that assumed by Almgren[37] but with a much smaller range of micelle size was used for the simulation, as defined by eq 9, viz.

$$f(N) = 0.1[\exp(-(N-1)/20) - \exp(-(N-1)/10)] \quad (11)$$

Likewise, the empirical formula used by Almgren to calculate how the intramicellar quenching rate constant might change with N was adapted to this smaller range of N. Even with this simplified starting point, it soon became apparent that the "crossing over" or common intersection of Infelta-type plots, as found in Figures 4−7, could not be reproduced. Instead, calculations produced a series of Infelta-type plots that exhibited parallel decays at all times. Subsequent analysis of these curves produced intramicellar rate constants that did not change with η. In fact, constant values of $A_4(k_q)$ were generated, rather than the variation in this parameter shown in the experimental data of the present study (Table 1 and Figure 8).

Further modeling of the original Almgren data (in which, at low N, k_q is about 10^8 s^{-1} and, at high N, k_q is about 5×10^5 s^{-1}) showed that the apparent k_q obtained from the fitting of the simulated fluorescence decay curves also changed very little, if at all, in comparison. Almgren's k_q changed, for example, only from 1.63×10^6 to 1.83×10^6 s^{-1}—reflecting perhaps a fixed weighted average value for k_q, with the small changes found arising from the variation in the goodness of fit of the simulated curves to an Infelta equation.

In retrospect, it seems clear that this kinetic model does not allow for the change in the probability of a quencher occupying a micelle as the proportion of occupied micelles becomes significant; i.e., the probability is fixed at $f(N)N$ regardless of the increasing occupancy of micelles by the quencher. In the Almgren simulation, for example, the average [pyrene]/[micelle] ratio, A_3, changes from 0.5 to 4.0 as η is increased from 1.25×10^{-3} to 1.0×10^{-2}, a significant degree of occupancy at all quencher concentrations. Similarly, in the current study where mean aggregation numbers of ∼10 were determined, the average occupancy varies from about 0.7 to about 1—also a significant degree of occupancy of micelles by the quencher. Further modeling is therefore required which takes into account the increasing occupancy of micelles as the amount of quencher in the system is increased. It may be anticipated that the aggregated intramicellar rate constant, calculated from a simulated fluorescence decay curve, will show much larger variations in magnitude depending on the type of distribution of micelle size assumed for the modeling. An exponential distribution, with large numbers of small micelles and a much smaller number of large micelles, should ensure that the smaller micelles are occupied preferentially at low quencher concentration, with consequential higher intramicellar aggregated rate constants. As [pyrene] is increased and relatively more of the larger micelles are occupied, the aggregated quenching rate constant will decrease. This predicted effect in the variation in k_q with η would be similar to that found in the current work and is likely to produce Infelta-type plots such as those found in Figures 4−7. For negatively skewed distributions with relatively high proportions of large micelles, it is anticipated that the opposite trend in k_q would be observed; i.e., an *increase* in k_q as [pyrene] increases. It is worth noting here that in a previous study on a C_{16} 35 kDa telechelic polymer,[24] using pyrene as quencher, that k_q was also found to decrease with increasing η. In this case, k_q decreased from 9×10^6 to 8×10^6 s^{-1}, as η increased from 0.001 to 0.016. When ethylpyrene was used as a quencher, the effect was even more marked. Here, k_q decreased from 1.4×10^7 to 1.0×10^7 s^{-1} as η increased from 0.001 to 0.016. No experimental plots were shown, however, so it was not possible to ascertain whether the characteristic intersection of fluorescence decay curves found in the current study was also observed in that study.

To date, there have been relatively few time-resolved fluorescence studies of telechelic associating polymers. Two of these involved polymers with a chain-extended PEG backbone to give M_w in the range 20.3−51 kDa. These polymers also had variable degrees of end-capping with n-C_{16} groups (0.96−1.7 hydrophobes/chain), the hydrophobes being derived from the corresponding alcohol and linked via coupling in the presence of isophorone diisocyanate.[13,34] There was no evidence of a polydisperse distribution of micelle sizes in these systems. Aggregation numbers of 18−28 were determined which decreased with increasing degree of hydrophobic substitution. One may speculate that the lack of polydispersity in micelle size is linked to the lower degree of terminal substitution—these materials more closely resembling nonionic surfactants on a simplistic level. Interestingly, the k_q values in these previous studies were up to a factor of 10 times lower than in the present work—values as low as 3×10^{-6} s^{-1} being observed. In this respect, there appears to be considerably more rigidity in these micelles. It has been speculated that the nature of the chemical linkage tethering the hydrophobes may have a role here, the bulky isophorone bridges contributing to the rigidity of the core. However, both the C_{16}-terminated polymers in these earlier studies[13,34] and the C_{12}-terminated polymer of this work contain identical isophorone bridges adjacent to the terminal hydrophobes. It would seem, therefore, that no simple correlation exists between the nature of the linking group and the rate of intermicellar quenching.

In another earlier study using a 20 kDa telechelic PEG end-capped with ether-linked n-C_{12} groups, a hydrophobe aggregation number of 28 ± 3 was determined using pyrene as a probe and dimethylbenzophenone (DMBP) as quencher.[33] Under these conditions, k_q was found to be about 3.6×10^7 s^{-1}. When pyrene was used as both probe and quencher, as in the current study, the aggregation number was found to be 15−16, at a η value of 0.05, with a corresponding k_q value of $(2.0 \pm 0.2) \times 10^7$ s^{-1}. Some evidence of polydispersity was perhaps evident in the DMBP studies where two different quencher concentrations at the same polymer concentration (3.76%) were investigated. However, the aggregation number, N_q, was found to decrease only slightly from 20 to 18 as the [DMBP]/[hydrophobe] ratio ($\equiv\eta$) increased from 0.045 to 0.085. At these relatively high values of η, the rate of decrease in the quencher average aggregation number is usually much smaller than for lower quencher concentrations [N_q is usually much more dependent on η in the range $\eta = 0.01-0.05$].[36] The aggregation number found for the DMBP experiment was higher than the values determined in the current study which yielded values in the range 10−16 for the $c = 1.5-2.5$ g dL^{-1} polymer solutions (see Figure 10). The latter values are however much closer to those found when pyrene was used as both quencher and probe.[33] It may be therefore that both of the pyrene self-quenching experiments in this work and in the previous study[33] are self-consistent when experiments at similar η values are considered, although one must also factor in the differences in M between the polymers. It could be that both of these telechelic systems are in fact polydisperse in micelle size. It is also worth noting that reasonably similar k_q values were found in both studies, using

pyrene as quencher, i.e., $(2.0 \pm 0.2) \times 10^7$ s^{-1},[33] compared to $\sim 1.0 \times 10^7$ s^{-1} in the present study.

Two other dynamic fluorescence studies of 35 kDa telechelic PEGs with simple urethane-linked *n*-C_{16} and *n*-C_{18} hydrophobic groups have been reported.[24,25] Here the parent PEG was end-capped by reaction with the corresponding alkyl isocyanates, thus avoiding chain extension of the backbone. Aggregation numbers of 16 and 21 were reported for the C_{16} polymer[24] and 23 for the C_{18} polymer.[25] In both of these studies, difficulties were experienced using the standard Poisson quenching model, requiring the development of an "extended" model to account for the data. It is clear, particularly for the C_{18} polymer study, that the data can be perhaps more easily interpreted in terms of polydispersity in micelle size. Thus, reconsidering this previously reported data, an alternative explanation would suggest an aggregation number decreasing from 122, at an η value of 0.005, to 20.5, at an η value of 0.1. The higher value (as $\eta \rightarrow 0$) would probably represent a value closer to the weight-average aggregation number, N_w. Selected data from one of these studies[25] are superimposed in Figure 10 for comparative purposes.

It has been shown theoretically that polydispersity in micelle size, arising from thermal fluctuations, for a C_{16} end-capped 35 kDa PEG is characterized by a skewed distribution in which the hydrophobe aggregation numbers are in the range 8−46, with number- and weight-average aggregation numbers of about 25 and 35, respectively.[32] For a C_{12} end-capped 35 kDa PEG a weight-average aggregation number of about 24 was predicted by these workers.

Our study has shown, in some detail, that micelles of a well-characterized C_{12} 35 kDa PEG polymer are substantially polydisperse in terms of aggregation number and more so than predicted by the above approach of Meng and Russel.[32] Either by extrapolation of the quencher average aggregation numbers, N_q, in Figure 10 to obtain a value at $\eta = 0$ or by assuming an exponential distribution of micelles and using eq 5 to fit the variation of experimental aggregation numbers with η, it seems that the weight-average aggregation number is ∼75. Pham et al.[30] also measured relatively high values of aggregation number for 35 kDa C_{16} and C_{18} telechelic polymers of 40 and 66, respectively—values, again, presumably close to the weight-average values. Our results, taken together with findings such as these, as well as the possibility of reinterpretation of previous dynamic fluorescence data[24,25] suggest strongly that polydispersity of micelle aggregation number is the normal expectation of telechelic associative polymers. Our dynamic fluorescence data have allowed a detailed study of polydispersity of a 35 kDa C_{12} telechelic PEG, where the theoretical approaches of Almgren[35,37] and Warr and Grieser[36] have been crucial to the understanding of the data. It may be anticipated that the issue of polydisperse aggregation numbers are of more significance than in the case of nonpolymer surfactants (e.g., lightly ethoxylated alcohols, SDS, etc.) and other similar hydrophobic systems where monodispersity seems to be the rule. The value of the dynamic fluorescence technique is thus clearly recognized. Other techniques such as static fluorescence,[23] small-angle neutron scattering,[27] and static light scattering provide aggregation numbers with differing weights and are also crucial in elucidating the detail of a polydisperse micellar system.

Conclusions

In conclusion, this study may be the first detailed time-resolved fluorescence study of the effect of polydispersity in micelle size of a telechelic associative polymer on the observed aggregation number (quencher average aggregation number, N_q). The values of the aggregation numbers found in the current study at η values ([quencher]/[hydrophobe]) above 0.05 are similar to those predicted by a theoretical treatment by Meng and Russel[32] and are also close to values found using techniques which determine mean or number-average aggregation numbers. The apparent value of the weight-average aggregation number, N_w, estimated in this work (∼75) is however much higher than the latter values and provide support for the high degree of polydispersity implied in this study. Such higher values have also been found, either intentionally[30] or perhaps unintentionally, through a reinterpretation of data by other workers.[24,25]

The importance of understanding the fundamental behavior of telechelic and other types of associative polymers is self-evident, if only for their wide industrial application and potential for development in other areas, such as healthcare. Our study has facilitated this understanding. It is equally clear, however, that there are areas where understanding needs to be improved. It is not clear, for example, why some apparently similar telechelic systems show little if any evidence of polydispersity of aggregation number[34] and why some systems show very rigid micellar cores. The role of the chemical linkage (e.g., ether, urethane, bridging bisurethane) between the hydrophilic backbone and the hydrophobic group may have some significant role and may be worthy of theoretical modeling in itself.

It would also appear that further theoretical modeling of associative polymers is essential for the prediction of the degree of polydispersity. The highly skewed micelle distribution supported by our dynamic fluorescence data is markedly different to the slightly skewed distribution predicted by Meng and Russel.[32]

Additionally, our attempts to model the pyrene fluorescence decay curves as attempted earlier for polydisperse surfactant systems[35,37] in order to get a detailed characterization of the micelle size distribution were not successful and have suggested that a better model, which takes into account the relative changes in the distribution of occupied micelles as quencher is added, should be developed. In this regard, it is noted that the earlier studies[35,37] were also not wholly satisfactory in this regard although crucial to the confirmation of polydisperse aggregation as an alternative explanation of the effect of quencher concentration on the decay kinetics of the probe's fluorescence.

Acknowledgment. The authors acknowledge the support of the UK Engineering and Physical Sciences Research Council (GR/S43771/01) and also of the CCLRC Free Radical Research Facility at Daresbury, Warrington, UK. We also extend our thanks to Lucy Miller and Natalie Davies of Welshpool High School, Powys, UK, who assisted in performing the light scattering and viscometry experiments supported by the 2006 Nuffield Foundation Bursary Scheme. We also acknowledge Prof. Mats Almgren and Dr. Mike Kasuba and colleagues for their kind advice and useful discussions in the preparation of this manuscript. Finally, we thank the reviewers for their constructive comments and Prof. Mitch Winnik for providing access to additional data from his previous work.

References and Notes

(1) Glass, J. E., Ed. *ACS Symp. Ser.* **1996**, *248*.
(2) Slater, G. W.; Kist, T. B. L.; Ren, H. J.; et al. *Electrophoresis* **1998**, *19*, 1525.
(3) Tonge, S. R.; Tighe, B. J. *Adv. Drug. Delivery Rev.* **2001**, *53*, 109.
(4) Taylor, K. C.; Nasr-El-Din, H. A. *J. Pet. Sci. Eng.* **1998**, *19*, 265.
(5) Yekta, A.; Aikawa, M.; Turro, N. J. *Chem. Phys. Lett.* **1979**, *63*, 543.
(6) Atik, S. S.; Nam, M.; Singer, L. A. *Chem. Phys. Lett.* **1979**, *67*, 75.
(7) Infelta, P. P. *Chem. Phys. Lett.* **1979**, *61*, 88.

(8) Infelta, P. P.; Graetzel, M.; Thomas, J. K. *J. Phys. Chem.* **1974**, *78*, 190.
(9) Binana-Limbele, W.; Zana, R. *Macromolecules* **1990**, *23*, 2731.
(10) Anthony, O.; Zana, R. *Macromolecules* **1994**, *27*, 3885.
(11) Anthony, O.; Zana, R. *Langmuir* **1996**, *12*, 3590.
(12) Zdanowicz, V. S.; Strauss, U. P. *Macromolecules* **1993**, *26*, 4770.
(13) Yekta, A.; Duhamel, J.; Brochard, P.; Adiwidjaja, H.; Winnik, M. A. *Macromolecules* **1991**, *26*, 182.
(14) Wilhelm, M.; Zhao, C-L.; Wang, Y.; Xu, R.; Winnik, M. A.; Mura, J-L.; Riess, G.; Croucher, M. D. *Macromolecules* **1991**, *24*, 1033.
(15) Noda, T.; Morishima, Y. *Macromolecules* **1999**, *32*, 4631.
(16) Noda, T.; Hashidzume, A.; Morishima, Y. *Langmuir* **2000**, *16*, 5324.
(17) Noda, T.; Hashidzume, A.; Morishima, Y. *Macromolecules* **2000**, *33*, 3694.
(18) Kumacheva, E.; Rharbi, Y.; Winnik, M. A.; Guo, L.; Tam, K. C.; Jenkins, R. D. *Langmuir* **1997**, *13*, 182.
(19) Horiuchi, K.; Rharbi, Y.; Spiro, J. G.; Yekta, A.; Winnik, M. A.; Jenkins, R. D.; Bassett, D. R. *Langmuir* **1999**, *15*, 1644.
(20) Araujo, E.; Rharbi, Y.; Huang, X.; Winnik, M. A.; Bassett, D. R.; Jenkins, R. D. *Langmuir* **2000**, *16*, 8664.
(21) Horiuchi, K.; Rharbi, Y.; Yekta, A.; Winnik, M. A.; Jenkins, R. D.; Bassett, D. R. *Can. J. Chem.* **1998**, *76*, 1779.
(22) Heyes, D. M.; Melrose, J. R. *J. Non-Newtonian Fluid Mech.* **1993**, *46*, 1.
(23) Elliot, P. T.; Xing, L.-L.; Wetzel, W. H.; Glass, J. E. *Macromolecules* **2003**, *36*, 8449.
(24) Vorobyova, O.; Yekta, A.; Winnik, M. A.; Lau, W. *Macromolecules* **1998**, *31*, 8998.
(25) Vorobyova, O.; Lau, W.; Winnik, M. A. *Langmuir* **2001**, *17*, 1357.
(26) Chassenieux, C.; Nicolai, T.; Durand, D. *Macromolecules* **1997**, *30*, 4952.
(27) Gourier, C.; Beaudoin, E.; Duval, M.; Sarazin, D.; Maitre, S.; Francois, J. *J. Colloid Interface Sci.* **2000**, *230*, 41.
(28) Beaudoin, E.; Borisov, O.; Lapp, A.; Billon, L.; Hiorns, R. C.; Francois, J. *Macromolecules* **2002**, *35*, 7436.
(29) Serero, Y.; Aznar, R.; Porte, G.; Berrer, J.-F; Calvet, D.; Collet, A.; Viguier, M. *Phys. Rev. Lett.* **1998**, *81*, 5584.
(30) Pham, Q. T.; Russel, W. B.; Thibeault, J. C.; Lau, W. *Macromolecules* **1999**, *32*, 2996.
(31) Preuschen, J.; Mechen, S.; Winnik, M. A.; Heuer, A.; Spiess, H. W. *Macromolecules* **1999**, *32*, 2690.
(32) Meng, X.-X.; Russel, W. B. *Macromolecules* **2005**, *38*, 593.
(33) Alami, E.; Almgren Brown, W.; Francois, J. *Macromolecules* **1996**, *29*, 2229.
(34) Yekta, A.; Xu, B.; Duhamel, J.; Adiwidjaja, H.; Winnik, M. *Macromolecules* **1995**, *28*, 956.
(35) Almgren, M.; Loefroth, J.-E. *J. Chem. Phys.* **1982**, *76*, 2734.
(36) Warr, G. G.; Gieser, F. *J. Chem. Soc., Faraday Trans. 1* **1986**, *82*, 1813.
(37) Almgren, M.; Alsins, J.; Mukhtar, E.; van Stam, J. *J. Phys. Chem.* **1988**, *92*, 4479.
(38) Petit-Agnely, F.; Iliopoulos, I.; Zana, R. *Langmuir* **2000**, *16*, 9921−9927.
(39) Navaratnam, S. In *Photostability of Drugs and Drug Formulations*; Tonnesen, H. H., Eds.; CRC Press: Boca Raton, FL, 2004; pp 255−284.
(40) Alargova, R. G.; Kochijashky, I. I.; Zana, R. *Langmuir* **1998**, *14*, 1575.
(41) Gehlen, M. H.; De Schryver, F. C. *Chem. Rev.* **1993**, *93*, 199.

MA0624649